Molecular Crystals and Liquid Crystals
Publication details, including instructions for authors and subscription information:
http://www.tandfonline.com/loi/gmcl20

Stimulated Raman Scattering of Dyes Under Random Lasing in Polymeric Vesicular Films

Vasil P. Yashchuk [a] , E. A. Tikhonov [b] & O. A. Prygodiuk [a]
[a] Faculty of Physics, Taras Shevchenko National University of Kyiv, Kyiv, Ukraine
[b] Institute for Physics, the NAS of Ukraine, Kyiv, Ukraine

Version of record first published: 03 Mar 2011

To cite this article: Vasil P. Yashchuk, E. A. Tikhonov & O. A. Prygodiuk (2011): Stimulated Raman Scattering of Dyes Under Random Lasing in Polymeric Vesicular Films, Molecular Crystals and Liquid Crystals, 535:1, 156-166

To link to this article: http://dx.doi.org/10.1080/15421406.2011.537971

Mol. Cryst. Liq. Cryst., Vol. 535: pp. 156–166, 2011

ISSN: 1542-1406 print/1563-5287 online
DOI: 10.1080/15421406.2011.537971

Taylor & Francis
Taylor & Francis Group

Stimulated Raman Scattering of Dyes Under Random Lasing in Polymeric Vesicular Films

VASIL P. YASHCHUK,[1] E. A. TIKHONOV,[2] AND O. A. PRYGODIUK[1]

[1]Faculty of Physics, Taras Shevchenko National University of Kyiv, Kyiv, Ukraine
[2]Institute for Physics, the NAS of Ukraine, Kyiv, Ukraine

The random lasing emission of dyed vesicular polymeric films under the diffusive regime of light propagation is investigated at helium temperature. It represents itself the coupling effect of the stimulated emission and the stimulated Raman scattering (SRS). Due to this effect, all the Raman lines are revealed in the random lasing spectrum. A distinguishing feature of the effect is that the stimulated emission (SE) promotes revealing the Raman lines. The intensity of Raman lines quadratically depends on the pumping intensity. Furthermore, the SRS under this condition has a more structured spectrum than the spontaneous Raman one. It makes it possible to detect even weak and closely located spectral lines.

Keywords Active Raman spectroscopy; dye; polymeric films; random lasing; stimulated Raman scattering; vesicles

Introduction

Recently, a specific nonlinear phenomenon—the coupling of the stimulated Raman scattering and the stimulated emission into a single process—was discovered in vesicular polymeric films with dyes rhodamine 6G and pyrromethene 597 [1,2].

Under a high pumping intensity, the stimulated emission of dye molecules in a medium with multiple scattering dominates over the spontaneous one. This leads to the lasing-like emission formation named the random lasing (RL). The spectrum of this emission depends on the scattering condition in a random media which is regulated by the ratio between the medium size l_m, mean scattering length $\overline{l_s}$, and emission wavelength λ.

In the diffusive mode of light propagation in a random medium ($l_m \gg \bar{l}_s \gg \lambda$), the scattered waves are incoherent and yield the total emission with a continuous spectrum. The lasing-like emission in this mode is formed as ASE (amplified spontaneous emission) with a continuous spectrum narrowed down to the minimal saturated value [3,4]. But, at a certain pumping intensity exceeding the random lasing threshold, the ASE spectrum of rhodamine 6G radically changes. The spectrum widens, and narrow

Address correspondence to Vasil P. Yashchuk, Faculty of Physics, Taras Shevchenko National University of Kyiv, Bldg. 1,2, Glushkov Ave., Kyiv, Ukraine. E-mail: yavasil@ukr.net

spectral lines arise against the continuous spectrum [1,2]. The spectral features of lines indicate that they are caused by the Raman scattering (RS). This gives the basic opportunity to study the Raman spectra from random lasing ones.

It is very actually for lasing dyes, because the powerful fluorescence often impedes the registration of weak RS signals. Last years, this problem was overcome by SERRS (surface enhanced resonance Raman spectroscopy) that increases the RS cross section, so that the RS signal becomes comparable with fluorescence ones. But this method needs a very low concentration of dye molecules to decrease the fluorescence. Therefore, the RS emission is weak and can be registered only with a special sensitive technique [5,6]. Another possibility to obtain the Raman spectra of lasing dyes is given by the inverse Raman scattering [7]. But this technique is even more complicated, because it requires two synchronized impulse sources of light: the pumping monochromatic source and the probing one with acceptable continuous spectrum in the anti-Stokes region. At last, Raman lines can be observed under SRS also, but the observation of Raman spectra in this case is impossible because only several frequencies (corresponding to modes with the highest Q) are revealed in this process.

Raman spectra obtained from the random lasing are free from these disadvantages. Neither complicated technique of registration nor specific light illumination is required. All what one needs are the scattering medium with the investigated dye, laser pumping, and single shot registration of radiation spectra. But, for the method to be applicable, one has to study the conditions of the formation of Raman spectra in the joint SE and SRS process and to analyze the features of these spectra. These problems are the subject of this paper.

Experimental

Samples and Instrumentation

We have investigated the random lasing spectra of the vesicular polymeric films dyed with rhodamine 6G and pyrromethenes 597 and 567. The films were fabricated from a nitrogen-containing ternary copolymer. The ethanol solution of dye (10^{-3}–$5 \cdot 10^{-3}$ M/l) was added to the solution of this copolymer and mixed. The films were deposited on a lavsan (dacron) substrate by coating with the dyed copolymer. Vesicles were generated after the film polymerization by UV illumination of homogeneous films and then fixed by heating. Under this condition, nuclei of gaseous nitrogen are created and then associated in vesicles. Their concentration depended on the UV illumination. Under a sufficient long-duration exposition, the vesicles are closely packed in the film plane. The mean diameter of vesicles was about 1.2 μm. The example of a microphoto (optical magnification 1000) of such vesicular film with rhodamine 6G under reflected illumination is shown in Figure 1.

The relative refractive index of vesicles in the polymer ($n = 1.5$) is as high as that of highly refractive particles (rutile, diamond, etc.) under the same conditions ($n = 1.6$). So, the high index and the close packing of vesicles ensure the effective light scattering in the sample plane, which is verified by a significant ($\approx$10 nm) long-wave shift of the luminescence spectrum maxima of a vesicular film relative to that of a homogeneous film (Fig. 2). This shift is caused by the enhanced reabsorption of a luminescence emission along the photon trajectory lengthened due to the multiple scattering. Then it may be considered as the evidence of a high scattering efficiency

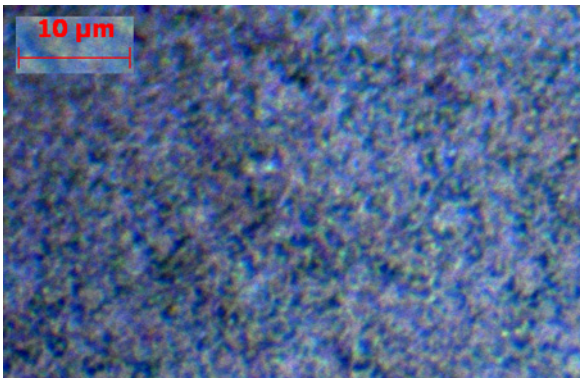

Figure 1. Microphoto of a rhodamine 6G dyed vesicular film under reflected light observation.

in the film. The mean diameter of vesicles (~1.2 μm) corresponds to the diffusive condition $\overline{l_s} \gg \lambda$ in the film plane.

The emission spectra of the sample were single-shot registered by means of a 1200-mm diffraction spectrograph (grating 1200 line/mm) and a CCD camera. The total spectral resolution was 0.2 nm. The emission spectra (lasing and luminescence) of films were registered in the backward direction. The image of a spectrum was displayed on a monitor and then digitized with a custom-made computer program. The program allows us to separate the linear Raman component of a spectrum from the continuous one caused by the random lasing.

The optical pumping of the sample was made by the second harmonic of a Q-switched YAG:Nd^{3+} ($\lambda = 532$ nm) laser. To verify whether the spectral lines are the RS ones, a tunable phosphate glass: Nd^{3+} laser was used instead of a YAG:Nd^{3+} one. The laser pulse durations were $\tau = 15$ ns and 25 ns, respectively. The pumping radiation is slightly focused at a sample, so the beam diameter at the front surface of

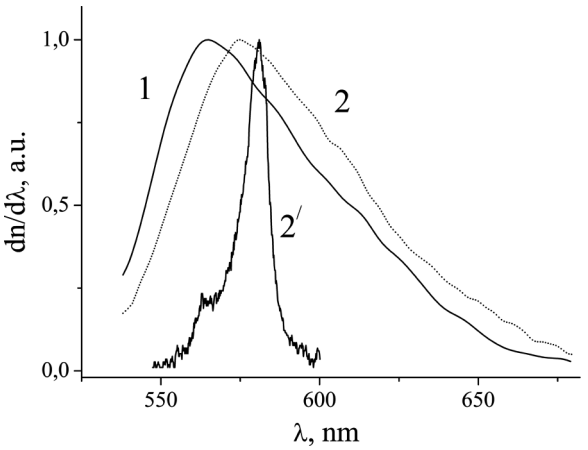

Figure 2. Shift of the fluorescence (2) and random lasing (2′) spectra of a vesicular area relative to the fluorescence spectrum of a homogeneous area (1) of the film with R6G.

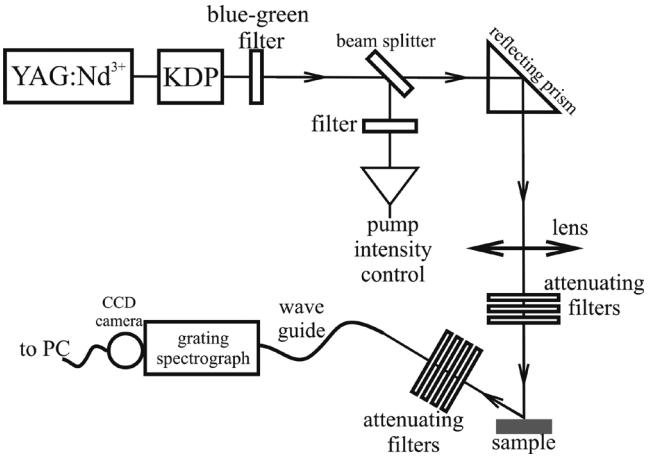

Figure 3. Outline of the setup to register the coupled emission of random lasing and stimulated Raman scattering.

the sample was $d = 1$ mm. The pumping intensity was varied with absorbing gray filters within the range $0.005 \div 0.5\,\mathrm{MW/mm^2}$.

To decrease the width of Raman lines and to shift the RL spectrum to the short-wave direction to overlap it with Raman lines, the experiments were performed at temperatures close to liquid helium ones (5–8 K). Other details of the experimental setup are shown in Figure 3.

Results and Discussion

The radiation spectrum of vesicular films at a rhodamine 6G concentration of about 10^{-3} M/l narrows to the saturation under the growth of the pumping intensity I_p up to a certain value I_{th} and then becomes invariable, as I_p increases further (Fig. 4,

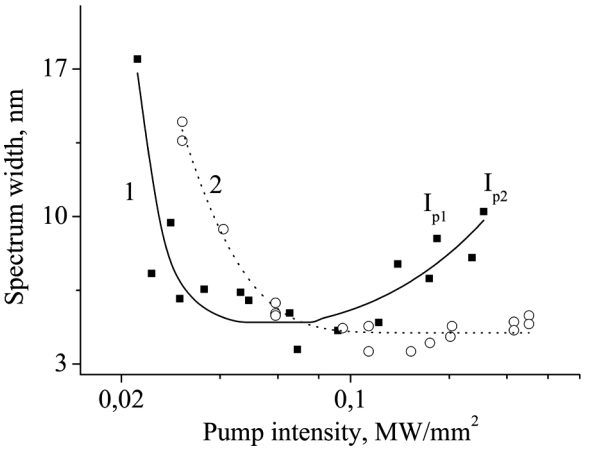

Figure 4. Dependence of the emission spectrum width of vesicular films on the pumping intensity for two R6G concentrations: $3 \cdot 10^{-3}$ M/l (1) and 10^{-3} M/l (2).

curve 2). The I_{th} value can be interpreted as the threshold pumping intensity of a random lasing [8]. It corresponds to the inflection point of the dependence of the spectrum width on the pump intensity $\Delta\lambda(I_p)$. Due to lower positive feedback efficiency, the spontaneous-to-lasing transition in a random laser is gradual (in contrast to the abrupt one in a conventional laser). The curve slope $\gamma = d(\Delta\lambda)/dI_p$ characterizes the rate of this transition. Values of I_{th} and γ depend on the dye concentration C_d: its increase results in a lowering of I_{th} and a growth of γ, which testifies to the better condition of RL.

It is remarkable that random lasing spectrum of the more dye concentrated film widens under RL threshold exceeding in several times (curve 1, Fig. 4). This spectrum widening is accompanied by the appearance of spectral lines against the continuous background of the RL spectrum (Fig. 5). Their intensities increase with the pumping, and their wavelengths are invariable and well reproducible from shot to shot. The films with a low dye concentration do not reveal this phenomenon: their spectra are invariable under the even more substantial exceeding of the RL threshold (curves 2, Fig. 4).

The absolute reproducibility of line wavelengths and the light diffusive propagation in the films indicate that the line structure of spectra is not due to the interference of scattered waves, but it is inherent in the investigated medium itself. The spectral lines in the RL spectrum are shifted under a variation of the pumping radiation wavelength in the strong accordance with its values [2]. The wavelengths of lines in the RL spectrum well coincide with ones of the Raman spectrum obtained by the SERRS method [5, 6] and by inverse Raman scattering [7]. These data prove explicitly the Raman scattering by dye molecules as the origination of lines in the RL spectrum of a film.

The number of Raman lines revealed in the RL spectrum depends on the spectrum width. The maximal RL spectrum width and thus the maximal number of Raman lines are revealed at the highest R6G concentration. The corresponding

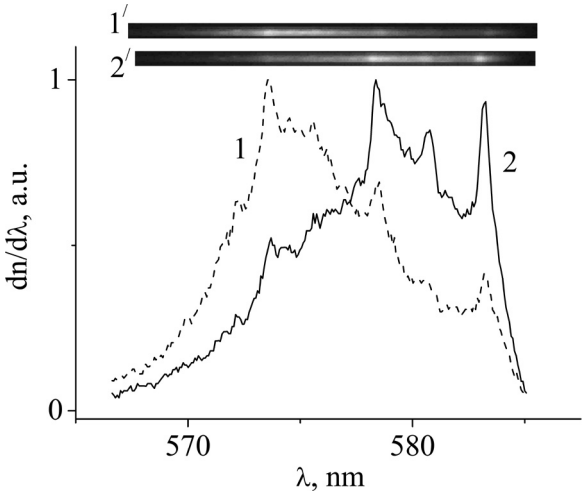

Figure 5. Lines in the spectrum (1, 2) and its CCD-images (1′, 2′) of a vesicular film at a high R6G concentration ($3 \cdot 10^3$ M/l) at the pumping intensities indicated as I_{p1}(1, 1′) and I_{p2} (2, 2′) in Fig. 4.

RL spectrum and a Raman spectrum separated from the first one are displayed in Figure 6a.

The answer to the question why the Raman scattering occurs at dye molecules, whose concentration is much lower than that of polymer matrix molecules, can be obtained from the dependence of the random lasing spectra on the dye concentration (Fig. 6b). The RL spectrum of R6G shifts against to C_d to the long-wave direction because of the enhanced reabsorption in the overlapping region of absorption and luminescence spectra. One can observe that Raman lines reveal themselves if they appear in the range of the RL spectrum only. The background of a random lasing spectrum corresponds to ASE, and it reproduces, in some approximation, the outline of the dye gain contour. Therefore, the background shift reflects the same shift of the dye gain and ASE contours. In this connection, the Raman lines are revealed in the random lasing only when these lines are disposed in the gain (ASE) contour. In this manner, the gain (ASE) contour "brightens" the Raman lines disposed in its range and makes them apparent.

Thus, the appearance of Raman lines in a random lasing spectrum is possible only when the dye molecules undergo the action of two emissions: pumping and random lasing (ASE) ones at Raman frequencies. Therefore, the intensity I_s of Raman lines (relatively to continuous background of a RL spectrum) is proportional to the product of random lasing I_{RL} and pumping I_p intensities. Since the value of I_{RL} is proportional to the pumping, the intensity I_s of Raman lines depends quadratically on I_p. It is clearly illustrated by the Raman lines in the RL spectrum of pyrromethene 597, where one of the lines (at $\lambda = 569.5$ nm) dominates over the other less intense ones (Fig. 7a). Due to this domination, the $I_s(I_p)$ dependence can be determined most accurately. One can see that the intensity of this Raman line depends quadratically on I_p with high accuracy.

The combined action of two mentioned radiations can be represented as a specific evidence of the active spectroscopy of Raman scattering (it more famous for anti-Stokes scattering as the CARS method – coherent anti-Stokes Raman

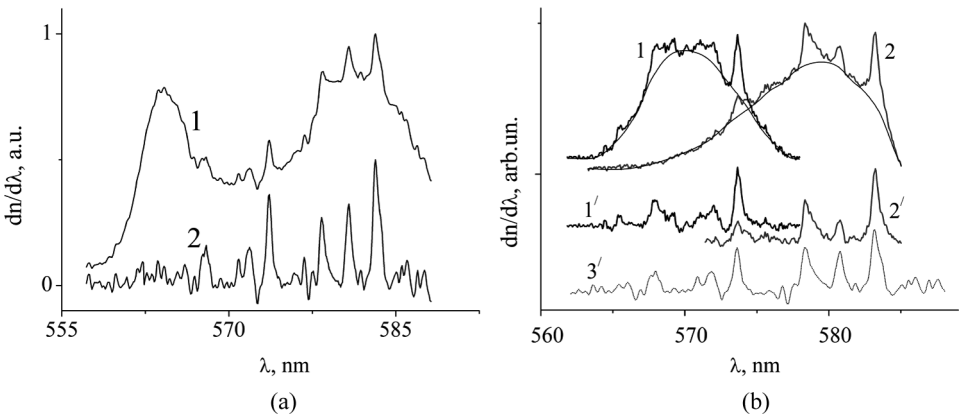

Figure 6. a) Spectra of the random lasing R6G of $5 \cdot 10^{-3}$ M/l (1) and the stimulated Raman scattering (2) separated from the first one; b) shift of the random lasing spectra and the gain contour (background) in compliance with the R6G concentration increase from 2 mM/l (1) to 3 mM/l (2) and the revealed sections of the dye spectrum: 1′—R6G: concentration is 2 mM/l, 2′—3 mM/l, 3′—whole Raman spectrum.

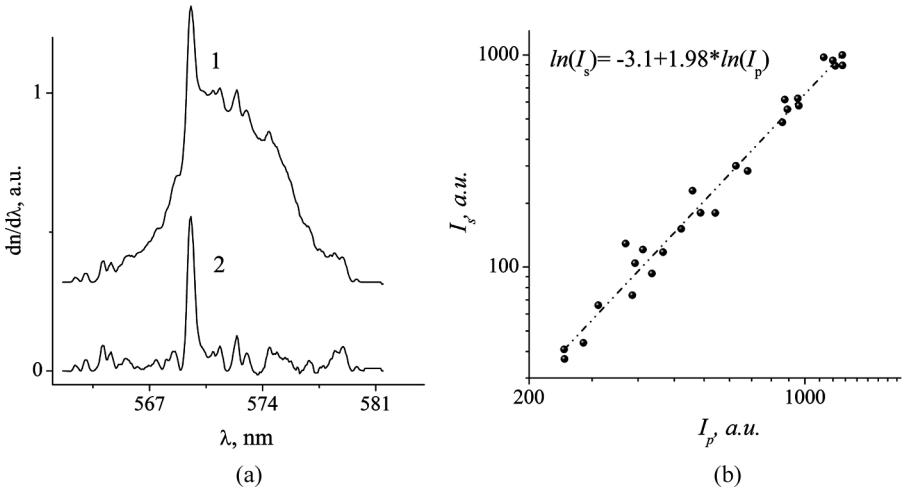

Figure 7. a) Random lasing (1) and Raman (2) spectra of pyrromethene 597 calculated from it; b) dependence of the most insensitive Raman line $\lambda = 569.5$ nm on the pumping intensity.

scattering), because the difference of their frequencies, ω_p (pumping radiation) and ω_s (random lasing at Raman frequencies), resonates with the vibration frequency ω_m of dye molecules and swings them [9]. In the conventional method, the samples are irradiated by a bichromatic pumping formed by two external monochromatic radiations: the base pumping with a fixed frequency ω_p and the additional one with a tunable frequency ω'. The Stokes scattering of the third (probing) monochromatic emission with frequency ω is investigated by the dependence on $\Delta\omega = \omega_p - \omega'$. This process can be conditionally depicted as $\omega_s = \omega - (\omega_p - \omega')$. The intensity of the scattered probing radiation depends on $\Delta\omega$ resonantly due to the third-order nonlinear susceptibility for SRS, $\chi^{(3)} \sim (\omega_m^2 - \Delta\omega^2 + 2i\Gamma\Delta\omega)^{-1}$, and reaches the maximum under the resonance condition $\Delta\omega = \omega_m$. In such a way, all the active Raman scattering frequencies are detected by turning the additional pumping frequency ω'.

In a strongly scattering active medium, the second (additional) component of a bichromatic pumping is created inside the sample by a separate process – the stimulated emission (random lasing) of dye molecules. The RL radiation is developed in a wide spectral range and serves as an additional pump at all Raman frequencies simultaneously. Owing to these peculiarities, no external bichromatic pumping is necessary. Only the single pumping monochromatic emission at a frequency ω is enough – the other (additional) one arises in the sample itself. There is no necessity of a special probing radiation also, because its role is played by the pump. Thus, in a strongly scattering medium, there is the degenerated case of the active spectroscopy of Raman scattering, in which the external (base) pump serves as a probing radiation as well, and the RL radiation at Raman frequencies serves as an additional pump: $\omega_s = \omega'$. Then this case can be conditionally depicted as $\omega_s = \omega_p - (\omega_p - \omega_s)$. Due to the continuous spectrum of RL in the diffusive mode, all Raman frequencies which occur in its contour can be manifested in the total radiation spectrum. From this point of view, the RL radiation (conditioned by ASE) is the additional pump with a broad spectrum, and then there is no necessity to tune its frequency. The SRS of dye molecules is resonant, because the pumping wavelength coincides with dye absorption

band. Therefore, the SRS probability for dye molecules is much higher than that for the matrix ones. For this reason, only the dye Raman lines can be observed in the RL emission.

Thus, the RL radiation of dyes in strong scattering media is determined by two processes: ASE and the amplified Raman scattering at all Raman frequencies occurring in the ASE spectrum. Respectively, the RL spectrum represents itself the sum of ASE (solid background) and the Raman scattering (lines) component. With this understanding, the radiation intensity I_{L} at the Raman frequency ω_s is the sum of the random lasing contribution I_{RL}(conditioned by ASE) and the Raman scattering one I_{S} (Fig. 8):

$$I_L = I_S + I_{RL} \tag{1}$$

The increments of I_{S} and I_{RL} per unit length can be described by the system of coupled differential equations [9, 10]

$$\frac{dI_S}{dz} = g \cdot \chi^{(3)}(\omega_S) I_p I_L, \tag{2}$$

$$\frac{dI_{RL}}{dz} = (\sigma(\omega_S) \cdot \Delta(I_p) - \alpha) I_L, \tag{3}$$

where $\chi^{(3)}(\omega_s)$ is the cubic nonlinear susceptibility at the Raman frequency ω_s (then $\Delta\omega = \omega_p - \omega_s$); g—proportionality coefficient depending on the Q factor of dye molecule vibrations; $\sigma(\omega_{\mathrm{s}})$—transition cross-section between the dye lasing levels; Δ—sample-averaged inverse population density; α—loss coefficient conditioned by the absorption and the sample overrunning of the radiation.

The solution of this system yields the expression for the radiation intensity exponentially depending on the cubic nonlinear susceptibility and the transition cross-section,

$$I_L = I_{L,0}(\omega_s, I_p) \exp\left(\left(g \cdot \chi^{(3)}(\omega_S) \cdot I_p + \sigma(\omega_S) \cdot \Delta(I_p) - \alpha\right) \cdot l\right), \tag{4}$$

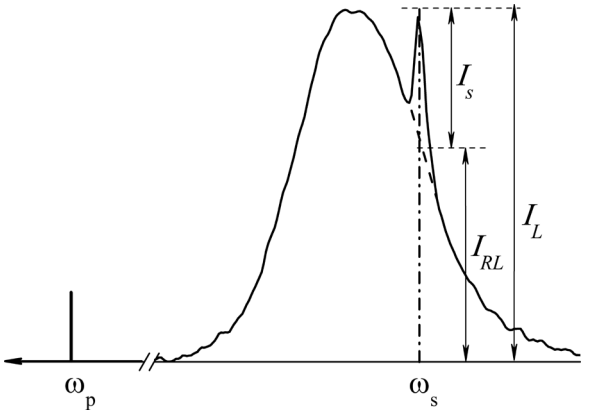

Figure 8. Components of the coupled emission in the random lasing: stimulated emission (ASE) I_{RL} and stimulated Raman scattering I_{s}.

where $I_{L,0}$—sample-averaged luminescence intensity. This expression is valid for any frequency (not only for a Raman one) because of the frequency-dependent parameters $\chi^{(3)}$ and σ. According to the formula, the RL spectrum is formed by coupling effects of the stimulated emission and the stimulated Raman scattering that yield a quasilinear spectral dependence of the gain coefficient:

$$k(\omega) = g \cdot \chi^{(3)}(\omega) \cdot I_p + \sigma(\omega) \cdot \Delta(I_p). \tag{5}$$

Owing to this dependence, the quasilinear contour of the RL spectrum is formed as a result of the amplification of the continuous luminescence spectrum $I_{L,0}(\omega)$. When the Raman line intensity is small ($I_S \ll I_{RL}$), the expression for the line intensity I_S can be derived from (4) and written as

$$I_S = g\chi^{(3)} I_{RL} I_p l \sim I_p^2, \tag{6}$$

where $I_{RL} \sim I_p$ [3, 8, 11]. Expression (6) agrees with the experimental dependence (Fig.7b) and, therefore, proves the adequacy of this consideration.

Expression (4) can be represented in the form

$$I_L(\omega) = I_{RL}(\omega) \cdot I_{SRS}(\omega), \tag{7}$$

where $I_{RL}(\omega)$ and $I_{SRS}(\omega)$ are the spectrum contours of RL (conditioned by ASE) and SRS, respectively, which are represented by the factors of relation (4):

$$I_{RL}(\omega) = I_{L,0}(\omega_s, I_p) \exp\big(\big(\sigma(\omega_S) \cdot \Delta(I_p) - \alpha\big)\big) \cdot l\big), \tag{8}$$

$$I_{SRS} = \exp\Big(g \cdot \chi^{(3)}(\omega_S) \cdot I_p \cdot l\Big). \tag{9}$$

Expression (7) allows finding the spectral dependence of the cubic susceptibility $\chi^{(3)}(\omega)$ as

$$\chi^{(3)}(\omega) \sim \ln I_{SRS}(\omega) = ln(\frac{I_L(\omega)}{I_{RL}(\omega)}). \tag{10}$$

This expression represented the SRS spectrum of dye molecules in arbitrary units. For a practical use of this formula, one needs to divide the total RL spectrum $I_L(\omega)$ (containing the ASE contour and the SRS spectrum) by the continuous background of it (corresponding only to ASE) and to take logarithm. To emphasize the way of obtaining the Raman spectrum, we denote this spectrum by SRS-RL. The result of this computation for R6G in comparison with the SERRS spectra obtained by two independent research teams [5,6] is shown in Figure 9a. For convenience, the maxima of spectral lines are linked with dashed lines. One can see that the computed SRS-RL spectrum agrees very well with SERRS ones. Almost all line frequencies of these spectra coincide with one another; their relative intensities are very close too. But the lines in SRS-RL spectra are sharper and better separated. Due to these peculiarities, several lines are resolved in the SRS-RL spectrum but are not resolved in SERRS ones (such as the lines with $\lambda = 565.3$, 566.1; 570.9, 571.9; 575.9, 576.9,

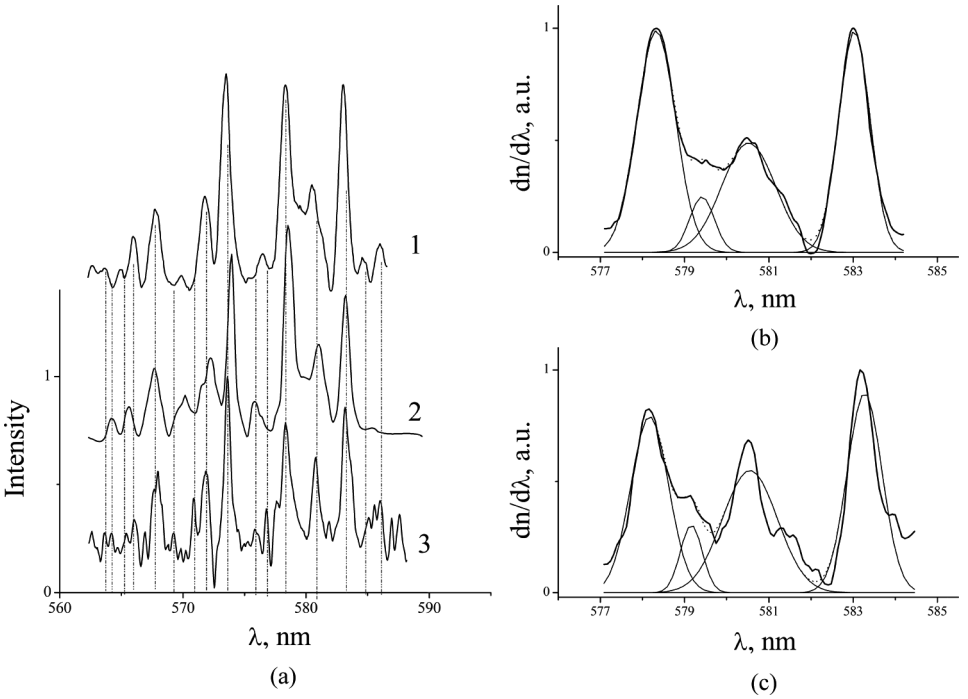

Figure 9. Comparison of SERRS (1 – [6], 2 – [5]) and SRS RL (3) spectra of R6G (a); decomposition of fragments of the SERRS ((b) – [6]) and SRS (c) spectra on the Gauss contours.

and 577.6 nm). The reality of these resolved components is confirmed by the IR absorption spectrum, where they are sufficiently intense [12].

This is more obvious from Figure 9b, c, where the decompositions of fragments of these spectra on Gauss bands are shown. The SERRS spectrum fragment is decomposed on four Gauss bands much better than the SRS-RL one. One can see that it is due to a better structurization of the SRS-RL spectrum as compared with that of the SERRS one. The lateral structure of the four lines in the SERRS spectrum fragment is barely noticeable. But, in the SRS-RL one, this structure is well observed. Owing to the better structurization of the SRS-RL spectrum, the fragment have to be decomposed on more Gauss bands to reach the same quantity of fitting as that of the SERRS spectrum – at least nine Gauss components. The SERRS spectrum is not a standard for the comparison because of the inhomogeneous broadening, but it is the best Raman spectrum of R6G (except the inverse Raman scattering) available now: conventional Raman spectra are not available due to the intensive luminescence of the dye. A better resolution of lines in the SRS-RL spectrum evidences of the perspective of this method for studying the Raman spectra.

The probable reason of a better structurization of the SRS-RL spectrum is the coherent nature of both emission mechanisms forming the RL spectrum: the stimulated emission and the stimulated Raman scattering. Owing to this coherence both radiations can interfere with each other and make the space between lines dipper like the interference of resonant and non-resonant components of the cubic nonlinear susceptibility of SRS in CARS [9]. The multiple scattering on vesicles destroys

partially the coherence of waves, but it might be kept at the space between two consequence scatterings. The Raman amplifying as another reason of the structurization can be excluded, because it does not influence the line contour in representation (10). In view of this circumstance, the electric field strengths of the ASE and Raman scattering waves should be summed in (1) instead of intensities. This approach is expected to describe the SRS-RL spectrum more precisely.

Summary

The random lasing of dyes in the diffusive mode represents itself the coupling effect of stimulated emission and stimulated Raman scattering. Due to this effect, all the lines active in Raman scattering can be revealed in the RL spectrum. The formula allowing the calculation of Raman spectra from SRS – RL spectra is obtained. The comparison of the Raman spectrum obtained in such a way with ones derived within other available methods has shown the adequacy of the new efficient method of registration of Raman spectra.

It is appreciable that the intensive luminescence does not impede the observation of Raman lines as the other methods do but promotes it, because the intensity of lines is proportional to the luminescence one. An important advantage of this method is a greater structurization of the SRS-RL spectrum caused by the coherent nature of the both coupled processes. This makes it possible to detect the weak and closely situated lines, as it is illustrated by Figure 9 and is confirmed by the IR absorption spectrum.

The peculiarities of this effect are very important for the lasing dyes spectroscopy because they allow one to study Raman spectra by means of RL spectra, which does not require a special technique. The liquid helium temperature promotes the observation of Raman lines, but it is not obligatory. For using this method, the strong scattering system with a dye has to be prepared only. In the present work, we have used the vesicular films which are very effective scattering systems, but the concentrated suspensions of dielectric particles (in polymer) are suited as well.

References

[1] Yashchuk, Vasil P., Tikhonov, E., Prigodiuk, O., Koreniuk, V., & Paskal, L. (2007). *Proc. of SPIE*, *6728*, 67280 N-1.
[2] Yashchuk, Vasil P., Tikhonov, E. A., & Prigodiuk, O. A. (2010). *JETP Letters*, *91*, 174.
[3] Lawandy, N. M., Balachandran, R. M., Gomes, A. S., & Sauvain, E. (1994). *Nature Lett.*, *368*, 436.
[4] van Soest, G., & Lagendijk, Ad. (2002). *Phys. Rev. E*, *65*, 047601–1.
[5] Zeng-Hui, Z., *et al*. (2006). *Chinese Physics*, *15*, 126.
[6] Meixner, A. J., Vosgrone, T., & Sackrow, M. (2001). *J. Luminescence*, *94–95*, 147.
[7] Lau, A., Vernike, V., & Pfafer, M. (1976). *Sov. Quant. Electr.*, *3*, 739.
[8] Tikhonov, E., Yashchuk, Vasil P., Prygodjuk, O., & Bezrodny, V. (2003). *Solid State Phenomena*, *94*, 295.
[9] Akhmanov, S. A., & Koroteev, N. A. (1977). *Sov. Phys. Usp.*, *20*, 899.
[10] Yariv, A. (1988). *Quantum electronics*. Wiley: New York.
[11] Kitur, J., Zhu, G., Bahoura, M., & Noginov, M. A. (2010). *J. Opt.*, *12*, 024009–1.
[12] Abd El Mongy, S. (2009). *Australian J. Basic and Appl. Sci.*, *3*, 1954 http://riodb01.ibase.aist.go.jp/sdbs/cgi-bin/direct_frame_top.cgi.